

## Zeeman Effect in the Absorption Spectrum of Copper-Doped Zinc Sulfide\*

M. DE WIT

*Texas Instruments Incorporated, Dallas, Texas 75222*

(Received 15 August 1968)

The Zeeman effect in the 1.44- $\mu\text{m}$  absorption line in copper-doped ZnS has been measured at liquid-helium temperature. Pure cubic ZnS was prepared in order to obtain a single absorption line. The Landé  $g$ -factor is  $0.71 \pm 0.02$  for the ground state. The excited state is observed to exhibit only a doublet structure in a magnetic field instead of a quartet structure. The  $g$  factor for this doublet is  $1.71 \pm 0.02$ . The measurements were made at 65 kOe. The Zeeman splittings are proportional to the field strength in the range 50–60 kOe. The angular dependence of the relative intensities of the observed transitions has been studied in an attempt to elucidate the nature of the excited state.

### I. INTRODUCTION

THE action of copper impurities in the luminescence of zinc sulfide and other II-VI compounds has been the subject of a large number of investigations.<sup>1</sup> In an attempt to study the structure of the Cu centers at the atomic level, a paramagnetic resonance study of Cu in ZnS has recently been made.<sup>2</sup> Although many paramagnetic resonance spectra of copper are seen, no paramagnetic copper center with tetrahedral symmetry has been seen by this technique. The measurement of the Zeeman effect of the optical absorption line believed to be due to copper in tetrahedral symmetry<sup>3</sup> is therefore reported here.

Briefly, in luminescence, copper gives rise to four types of centers which are responsible for the blue, green, red, and infrared luminescence bands. Of these, the infrared band is of special interest here because careful studies by Broser and coworkers<sup>3</sup> have clarified a number of features of this band. First, the generation of the Cu center by transmutation of zinc gives strong evidence that the center is  $\text{Cu}_{\text{Zn}}$  and no further association with another defect is involved. Second, the infrared luminescence bands have been resolved into a number of sharp lines, and absorption lines corresponding to luminescence lines have been identified. Third, when the center is obtained in pure cubic material, only one sharp line is observed in absorption and two closely spaced lines in emission. The single absorption line

indicates that the center has tetrahedral symmetry. One of the emission lines is at the same energy,  $6927 \text{ cm}^{-1}$ , as the absorption line and the second occurs  $14 \text{ cm}^{-1}$  lower in energy. The observed transitions in microscopically twinned cubic material and the energies of the transitions all seem consistent with the simplest model of the  $3d^9$  configuration of  $\text{Cu}_{\text{Zn}}$  in ZnS. The optical absorption corresponds to the cubic crystalline-field splitting of the  $3d^9$  configuration, modified by the spin-orbit interaction.<sup>3</sup> This charge state of Cu is paramagnetic, but the lines in twinned material are too close together to allow an unambiguous Zeeman-effect measurement. The work reported on here is the Zeeman effect of the absorption line in pure cubic material. The results do not agree with the simple crystal-field model. The excited state which is a quartet according to the model, splits as a doublet in a magnetic field. Large shifts of the  $g$  factors away from the simple model prediction of 2 are found to occur. Although such a shift in the ground state may be attributed to covalency effects,<sup>4</sup> or more likely, to the presence of the dynamic Jahn-Teller<sup>5</sup> effect, its presence in the excited state has not been explained. Section II is a description of a little-known method used to prepare pure cubic ZnS crystals. Section III describes the optical measurements, and in Sec. IV the crystal-field model is examined in the light of the experimental results. The Jahn-Teller effect is discussed qualitatively in the discussion of Sec. V.

### II. EXPERIMENT

The single crystals used in this work were grown in an HCl transport reaction.<sup>6</sup> Such crystals are twinned on a microscopic scale with two cubic regions rotated  $60^\circ$  with respect to each other about the  $[111]$  growth direction and with some sort of transition region of hexagonal character separating them. The infrared luminescence bands at 1.65 and 1.5  $\mu\text{m}$  in powders<sup>1</sup> or the zero-phonon lines<sup>3</sup> in the range 1.43–1.47  $\mu\text{m}$  in

\* Research sponsored in part by the Air Force Office of Scientific Research Contract No. F-44620-67-C-0073.

<sup>1</sup> For recent reviews see S. Shionoya, in *Luminescence of Inorganic Solids*, edited by Paul Goldberg (Academic Press Inc., New York, 1966), Chap. 2, p. 206; D. Curie and J. S. Prener, in *Physics and Chemistry of II-VI Compounds*, edited by M. Aven and J. S. Prener (John Wiley & Sons, Inc., New York, 1967), Chap. 9, p. 435.

<sup>2</sup> W. C. Holton, M. de Wit, R. K. Watts, T. L. Estle, and J. Schneider, (to be published); T. L. Estle, W. C. Holton, M. de Wit, R. K. Watts, A. R. Reinberg, and J. Schneider in Proceedings of the International Conference on Luminescence, Budapest, 1966 (to be published).

<sup>3</sup> I. Broser and K. H. Franke, *J. Phys. Chem. Solids* **26**, 1013 (1965); I. Broser, H. Maier, and H.-J. Schulz, *Phys. Rev.* **140**, A2135 (1965); I. Broser and H. Maier, *J. Phys. Soc. Japan Suppl.* **21**, 254 (1966); I. Broser, K.-H. Franke, and H.-J. Schulz, in *II-VI Semiconducting Compounds 1967 International Conference*, edited by D. G. Thomas (W. A. Benjamin, Inc., New York, 1967), p. 81.

<sup>4</sup> K. W. H. Stevens, *Proc. Roy. Soc. (London)* **A236**, 549 (1956).

<sup>5</sup> H. A. Jahn and E. Teller, *Proc. Roy. Soc. (London)* **A161**, 220 (1937); F. S. Ham, *Phys. Rev.* **138**, A1727 (1965).

<sup>6</sup> F. Jona, *J. Phys. Chem. Solids* **23**, 1719 (1962); and H. Samelson, *J. Appl. Phys.* **33**, 1779 (1962).

microscopically twinned crystals are associated primarily with the copper impurities situated within the transition region between the cubic parts. Only in pure cubic crystals does a single absorption line appear.<sup>3</sup>

Pure cubic material may be grown with a modified furnace. A tap is provided at the center of the gradient region and the hot end is kept at 1100°C but the cold end is oscillated from 930 to 950°C once per hour.<sup>7</sup> The transport is completed in about 5 days. The crystals usually are platelets but are now macroscopically twinned parallel to the large face, which sometimes is a (110) plane, but more often is a (111) plane. The platelets are ground down to the single-crystal region and polished for the optical work. The crystals are clear as grown and show the self-activated blue luminescence under uv excitation. Occasionally contamination occurs, frequently with Cu, and the crystals exhibit a green cast in fluorescent room lighting. The large dimensions of the crystals obtained this way are 0.5 cm or less and thicknesses are a few mm. The crystals were doped in a diffusion process. The copper metal was evaporated on the crystal and a first heating was performed in vacuum for 100 h. Temperatures in the range 400–800°C, which are well below the cubic to hexagonal transition temperature of 1020°C,<sup>6,8</sup> were used. The infrared absorption is usually not observed after this treatment. The crystals are then heated in a sulphur atmosphere at 530°C for 100 h. The crystals are now grey in appearance and if necessary are polished down on one side to an optical density of about unity. Since these are halogen-transported crystals, a weak Cu green luminescence appears under ultraviolet excitation. The infrared luminescence typical of the luminescent powder was not observed in these single crystals under broad-band excitation.

The Cu concentration in one sample was determined to be 0.1% by emission spectrometry and if all the Cu contributes to the infrared absorption line, an oscillator strength of  $10^{-4}$  is computed for this transition.

The Zeeman-effect experiments were performed at the Magnet Facility of the Southwest Center for Advanced Studies. The magnet used was a Bitter solenoid with radial access and 65-kOe maximum field. Simple optics with a beam aperture of  $f/10$  were used and the light propagated perpendicular to the field. The sample was immersed in liquid He together with the polarizer since the Dewar windows were unoriented sapphire. The light was a 650-W tungsten-iodine projector lamp. The light was passed through the sample and then analysed with a 0.5-m Jarrel-Ash spectrometer with a 295-lines/mm grating and curved slits. No other filtering of the light was used. The signal was detected with a cooled PbS detector and the signal-to-noise ratio was detector-limited. The resolution was set at 4 Å to obtain sufficient light on the detector and yet not broaden the

absorption line. The amount of power incident on the sample was 0.1–0.3 W. Most of this energy is absorbed by the sample which has an optical density of about 1.0 throughout the region of the lamp emission. As a consequence, the sample temperature is about 4°K when the bath is pumped to the  $\lambda$  point or 8°K when the bath is at 4.2°K. The sample temperatures were determined from the relative population of the two Zeeman-split ground-state levels.

The water-vapor absorption in the atmosphere was used to establish a wavelength scale. Where the individual lines are not resolved, the predicted intensities were used and the average line position was computed from tables.<sup>9</sup>

### III. RESULTS

In zero magnetic field the linewidth is typically  $1.5 \text{ cm}^{-1}$  at  $6926 \text{ cm}^{-1}$  at liquid-He temperature. At 20–30°K the line has broadened to  $3.6 \text{ cm}^{-1}$  and its amplitude has decreased some four times. The spectrum is unobservable at 77°K and the present measurements are all made with the He bath pumped to the  $\lambda$  point. The light is incident along the  $[1\bar{1}0]$  direction and the orientation of the Zeeman field  $\mathbf{H}_0$  could be varied in the  $(1\bar{1}0)$  plane. Figure 1 shows the spectrum at 65.6 kOe with  $\mathbf{H}_0 \parallel [001]$  and unpolarized light. Of the six lines in the figure the outer two are water vapor and are used for wavelength calibration. The four lines that belong to the copper originate from transitions between two levels in the ground state and two levels in the excited state. There is no evidence that the lines broaden when the magnetic field is applied. The intensity ratio of the various lines changes as the sample temperature is varied and has its origin in the relative population of the two ground-state levels. The splittings indicated

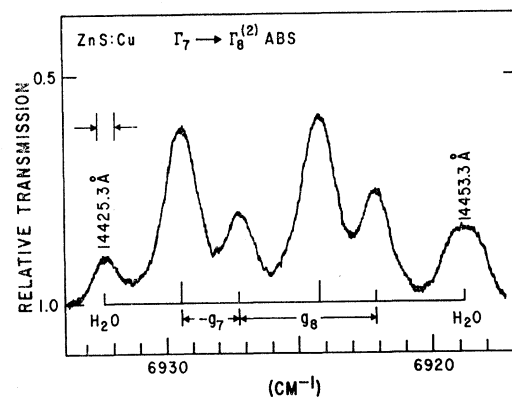


FIG. 1. Relative transmission of ZnS:Cu at liquid-helium temperature for unpolarized light propagating along  $[1\bar{1}0]$ . The Zeeman field is 65.6 kOe and is along the  $[001]$  direction. Of the six lines shown the two outer lines are due to water vapor absorption in the atmosphere. The resolution is indicated in the left side of the figure. The splittings  $-g_7$  and  $g_8$  are in the ground and excited states, respectively.

<sup>7</sup> H. Schafer, *Chemical Transport Reactions* (Academic Press Inc., New York, 1964), p. 87.

<sup>8</sup> E. T. Allen and J. L. Crenshaw, *Am. J. Sci.* **34**, 341 (1962).

<sup>9</sup> O. C. Möhler, *A Table of Solar Spectrum Wavelengths* (The University of Michigan Press, Ann Arbor, 1955).

by  $-g_7$  and  $g_8$  in Fig. 1 are then the Zeeman splittings of the ground state and excited state, respectively. The transition is assumed to be the  $d$  to  $d$  transition within the cubic crystal-field split  $3d^9$  configuration. As discussed in Sec. IV, crystal-field theory predicts that the ground state is a Kramers doublet  $\Gamma_7$  and the excited state is a quartet  $\Gamma_8^{(2)}$ , which to a first approximation consists of two Kramers doublets with equal Landé  $g$  factors. This energy-level structure is shown in Fig. 2. The electric dipole transitions that originate from the lower ground-state level are indicated with the polarization selection rules when the field is along  $[001]$ . The Zeeman splitting of a Kramers doublet is isotropic in cubic symmetry but the splitting of a  $\Gamma_8$  quartet need not be in general.<sup>10</sup> In an attempt to determine the quartet nature of the excited state an angular dependence of the Zeeman splitting on the field orientation was

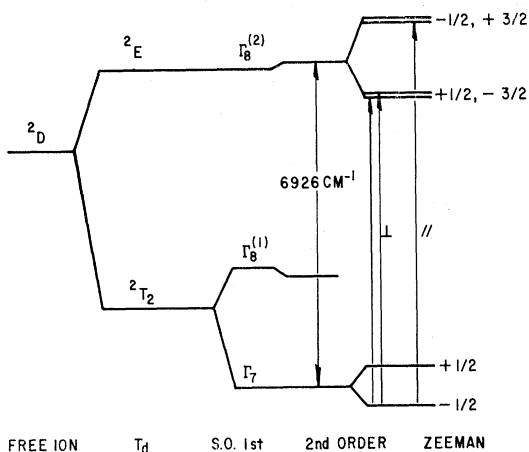


FIG. 2. Energy-level diagram of the  $3d^9$  configuration in tetrahedral symmetry. Electric dipole transitions from the lower level of the ground state are shown for the electric vector parallel and perpendicular to the Zeeman field, when the latter is along  $[001]$ .

searched for. However, no significant variation was detected. A slight variation was found in both  $g_7$  and  $g_8$  but was comparable to the scatter in these values. The variation was, therefore, attributed to a systematic uncertainty. The 19 measurements were averaged and the result for the ground state is  $|g_7| = 0.71 \pm 0.02$  and for the excited state  $|g_8| = 1.71 \pm 0.02$ . This uncertainty is 1/20 of the linewidth at half-maximum and the scatter of the points including the systematic shift is  $\frac{1}{5}$  of the linewidth. Measurements at 50 kOe show that the Zeeman effect is linear in the field strength.

The relative intensities of the lines vary as the crystal is rotated in the field. This variation is plotted as the ratio of the total intensity  $I_0$ , of the outer pair of lines in Fig. 1, to that of the inner pair  $I_i$ . This is shown in Fig. 3, when  $\mathbf{H}_0$  is in the  $(1\bar{1}0)$  plane and makes an angle  $\theta$  with  $[001]$ . The curves  $e$  and  $m$  are the pre-

<sup>10</sup> Y. Ayant, El Belorizky, and J. Rosset, J. Phys. Radium 23, 14 (1962).

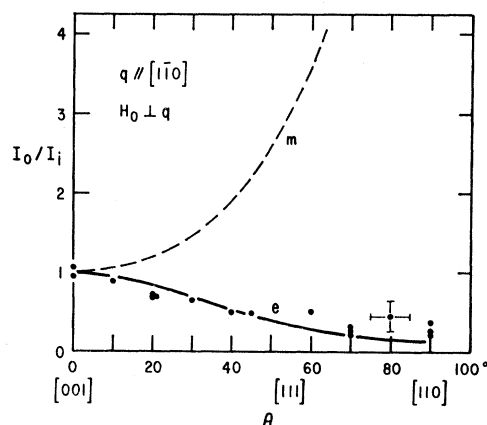


FIG. 3. Angular dependence of the ratio of the total intensity  $I_0$  in the outer pair of lines of Fig. 1 to that of the inner pair  $I_i$ . The Zeeman field is in the  $(1\bar{1}0)$  plane. Curves  $e$  and  $m$  are the crystal-field predictions for electric dipole and magnetic dipole transitions.

dicted angular behavior for electric dipole and magnetic dipole transitions according to crystal-field theory as discussed in Sec. IV.

A similar set of measurements was performed with polarized light and Figs. 4 and 5 show the results when the electric field vector is parallel to the Zeeman field. Figures 6 and 7 show the results when the electric vector is perpendicular to the Zeeman field.

#### IV. CRYSTAL-FIELD MODEL

We shall attempt to interpret the spectrum with the simplest possible model, that of isolated substitutional copper. This is the  $3d^9$  configuration in a crystal field of tetrahedral symmetry. In addition, the spin-orbit interaction is included and also covalent bonding. The

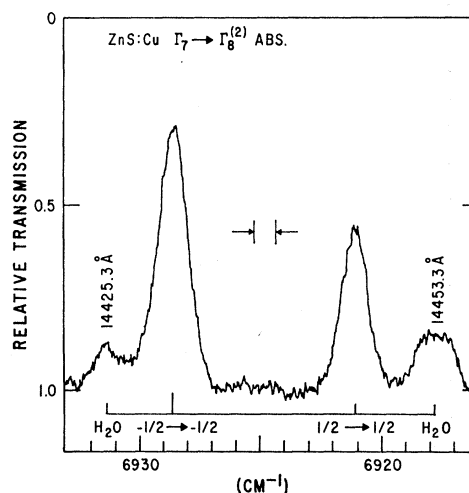


FIG. 4. Absorption spectrum at liquid-helium temperature when the electric vector of the light beam is parallel to the Zeeman field, which is along the  $[001]$  direction. The field is 65.8 kOe and the light propagates along  $[1\bar{1}0]$ . The transitions are labeled according to Fig. 2.

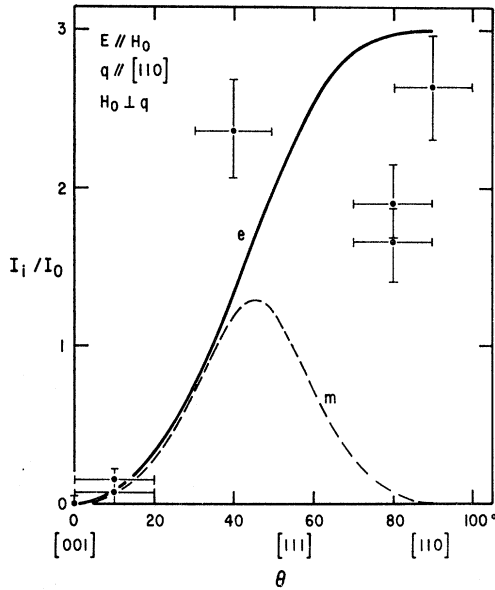


FIG. 5. Angular dependence of the ratio of the total intensity of the inner pair of lines to that of the outer pair, when the electric vector is parallel to the Zeeman field.

latter is included because it provides a mechanism which reduces the orbital contribution to the magnetic moment in the ground state. The energy levels in this approximation are well known and shown in Fig. 2. The theory has been worked out in some detail for a related symmetry by Dietz *et al.*<sup>11</sup> The ground state in a  $\Gamma_7$  Kramers

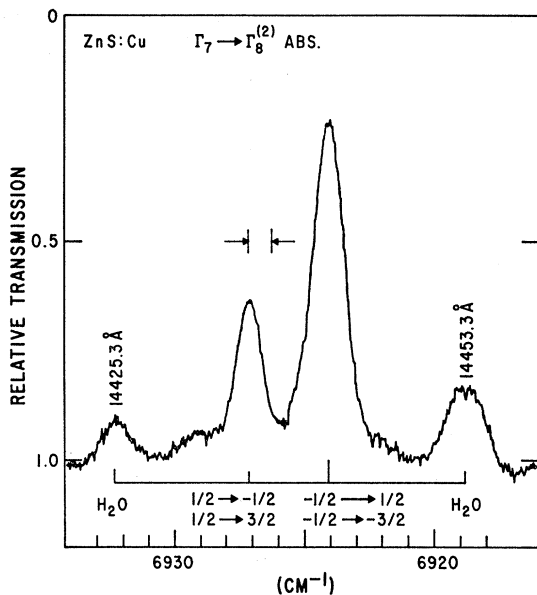


FIG. 6. Same as Fig. 4 except that the electric field of the light is perpendicular to the Zeeman field.

<sup>11</sup> R. E. Dietz, H. Kamimura, M. D. Sturge, and A. Yariv, *Phys. Rev.* **132**, 1559 (1963).

douplet and the Landé factor is

$$g_7 = -(4k+2)/3, \tag{1}$$

where  $k$  is the orbital reduction factor<sup>4</sup> which may range from 0 to 1 in the covalent  $\sigma$ -bonding model.<sup>11</sup> The two excited states are both  $\Gamma_8$  quartets and the absorption spectrum corresponds to the transition to the upper one, i.e.,  $\Gamma_7 \rightarrow \Gamma_8^{(2)}$  at  $6926 \text{ cm}^{-1}$ . This energy is the sum of the crystal-field splitting  $10 Dq$  and the spin-orbit interaction energy  $-\lambda \approx 850 \text{ cm}^{-1}$ . The upper  $\Gamma_8$  quartet has a peculiar nature in that it behaves as two independent Kramers doublets when the second-order spin-orbit interaction is neglected. This is related to the  $d$  functions from which the four levels are derived. The wave functions of the states labeled  $M = \pm \frac{1}{2}$  are proportional to  $\pm Y_{20} \chi_{\pm 1/2}$ . The  $Y_{lm}$  is the spherical harmonic which appears in the  $d$  function and  $\chi_n$  is the spin- $\frac{1}{2}$  function. The states  $M = \pm \frac{3}{2}$  are proportional to

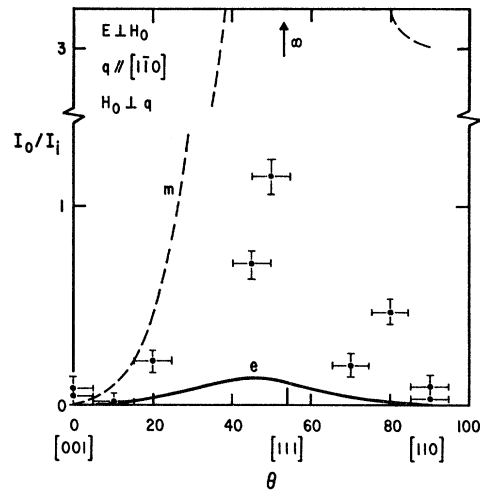


FIG. 7. Same as Fig. 5 except that the electric field of the light is perpendicular to the Zeeman field.

$\mp (Y_{22} + Y_{2-2}) \chi_{\mp 1/2}$ . The matrix elements of the orbital angular momentum  $\mathbf{L}$  all vanish within these four states. On the other hand the nonvanishing matrix elements of the spin only connect states within each  $\pm M$  doublet. The  $g$  factor for each doublet, therefore, has the spin only value of 2. These results are modified somewhat when the interaction between the two  $\Gamma_8$  quartets is taken into account. When the magnetic field is a long the  $[001]$  direction the  $g$  factors are

$$g_8(\pm \frac{1}{2}) = 2N^2, \tag{2}$$

$$g_8(\pm \frac{3}{2}) = -[2N^2 + \sqrt{4\frac{2}{3}\alpha N - \frac{2}{3}\alpha^2}],$$

where the  $\Gamma_8^{(1)}$  quartet is admixed into the  $\Gamma_8^{(2)}$  quartet in the ratio of  $\alpha:1$  and  $N$  is the renormalization of the  $\Gamma_8^{(2)}$  wave function. When the admixture takes place by means of the spin-orbit interaction these

expressions are, to second order in perturbation theory,

$$\begin{aligned} g_8(\pm\frac{1}{2}) &= 2, \\ g_8(\pm\frac{3}{2}) &= -[2-8\lambda/(10Dq)]. \end{aligned} \quad (3)$$

The simple model predicts the electric dipole transitions which are indicated in Fig. 2, i.e.,  $\Delta M=0$  when  $\mathbf{E}\parallel\mathbf{H}_0$  and  $\Delta M=\pm 1$  when  $\mathbf{E}\perp\mathbf{H}_0$ . Electric dipole  $nd$ -to- $nd$  transitions may occur in tetrahedral symmetry because of the lack of inversion symmetry in this point group and hence the lack of a parity selection rule. The term in the crystal-field potential proportional to  $xyz$  admixes the  $p$  functions, which form a  ${}^2T_2$  term, with those  $d$  functions of the same symmetry. The calculated intensities of the transitions  $\frac{1}{2}\rightarrow\frac{1}{2}$ ,  $\frac{1}{2}\rightarrow-\frac{1}{2}$ ,  $\frac{1}{2}\rightarrow\frac{3}{2}$  are in the ratio  $1:\frac{1}{4}:\frac{3}{4}$  when the Zeeman field is along  $[001]$  and the light is unpolarized. There should be two transitions with  $\Delta M=\pm 1$ ; however, only one is observed with an intensity equal to that of the  $\Delta M=0$  transition. This indicates that in the model the levels  $+\frac{1}{2}$  and  $-\frac{3}{2}$  of  $\Gamma_8^{(2)}$  are coincident. The general theory of the  $\Gamma_8$  quartet<sup>10</sup> shows that if these levels are coincident the Zeeman splitting shows no angular dependence when the magnetic field is in the (110) plane. This is consistent with our observations.

The polarization selection rules are quite accurately obeyed for the field along  $[001]$  and the transitions in Figs. 4 and 6 have been labeled according to the notation in Fig. 2. The spectrum in Fig. 1 and the polarization selection rules can only be obtained with electric dipole transitions when  $g_7$  and  $g_8(\pm\frac{1}{2})$  have opposite sign, i.e., the ordering of the levels  $M=\pm\frac{1}{2}$  of  $\Gamma_8^{(2)}$  is opposite to that in  $\Gamma_7$ . If this ordering is the same in ground and excited state, the results for  $\mathbf{H}_0\parallel[001]$  fit a magnetic dipole transition. In this case, the  $\Delta M=\pm 1$  transitions occur for  $\mathbf{E}\parallel\mathbf{H}_0$  and  $\Delta M=\pm 2$  for  $\mathbf{E}\perp\mathbf{H}_0$ . The total intensity of the transitions for each polarization is again equal. However, the angular dependence of the relative intensities of the lines show the difference between electric and magnetic dipole transitions more clearly. This has been calculated in terms of the ratio of the intensity of the outer pair of lines  $I_0$  to that of the inner pair  $I_i$ . For an electric dipole transition  $I_0$  is proportional to the transition probability  $P(\frac{1}{2}\rightarrow\frac{1}{2})$  and  $I_i\propto P(\frac{1}{2}\rightarrow-\frac{1}{2})+P(\frac{1}{2}\rightarrow\frac{3}{2})$ . The expressions are plotted in Figs. 3, 5, and 7 as curve  $e$  and are

$$\begin{aligned} I_0/I_i &= (3C^2+1)/(7-3C^2), \\ I_i/I_0 &= (1+C^2)/3(1-C^2)(1+3C^2), \quad \mathbf{E}\parallel\mathbf{H}_0 \\ I_0/I_i &= C^2(1-C^2)/[4-9C^2(1-C^2)], \quad \mathbf{E}\perp\mathbf{H}_0 \end{aligned} \quad (4)$$

where  $C=\cos\theta$  and  $\theta$  is the angle between the  $[001]$  crystal axis and the Zeeman field when the field is rotated in the (110) plane. For the magnetic dipole transition the order of the levels in the ground state are arbitrarily reversed and  $I_0\propto P(\frac{1}{2}\rightarrow-\frac{1}{2})+P(\frac{1}{2}\rightarrow\frac{3}{2})$  and  $I_i\propto P(\frac{1}{2}\rightarrow-\frac{3}{2})$ . The expressions are plotted in

Figs. 3, 5, and 7 as curve  $m$  and are

$$\begin{aligned} I_0/I_i &= (7-3C^2)/(1+3C^2), \quad \text{unpolarized} \\ I_i/I_0 &= 9C^2(1-C^2)/(9C^4-9C^2+4), \quad \mathbf{E}\parallel\mathbf{H}_0 \\ I_0/I_i &= [4-(3C^2-1)^2]/(3C^2-1)^2, \quad \mathbf{E}\perp\mathbf{H}_0. \end{aligned} \quad (5)$$

In the calculation of these expressions, the second-order interaction between the two  $\Gamma_8$  quartets has been neglected. In comparing the observation with the calculated curves they fit qualitatively to the electric dipole transition model and hence a negative  $g$  factor in the ground state.

The observations on the  $g$  factors are poorly explained with the expressions (1), (2), or (3). In the ground state we find  $h=0.03$ , i.e., essentially complete orbital reduction. If this orbital reduction is attributed to covalent bonding it would correspond to a ten times higher electron density on the four sulfur ligands than on the central Cu ion. Such a large delocalization is inconsistent with the approximations implicit in the covalent-bonding model and probably also with the crystal-field model for systems with energy levels 1 eV or more from the band edge. Another possible origin of the orbital reduction factor is in the Jahn-Teller effect, where these large reductions of the orbital angular-momentum matrix elements are a consequence of the small overlap of the nuclear parts of the wave function (Ham effect)<sup>5</sup> and fit easily within the framework of the crystal-field model.

The excited-state splitting is more difficult to fit with the simple model. The results shown in Figs. 1, 4, and 6 show no indication of a splitting of the inner pair of lines and the two Kramers doublets of the excited state must therefore coincide. Even if the two transitions which contribute to each of the inner pair of lines were separated by less than the linewidth, such that no appreciable broadening of the line would be observed, the height should be less than the for outer pair of lines. If the  $-\frac{1}{2}\rightarrow+\frac{1}{2}$  transition which has a relative intensity of  $\frac{1}{4}$  is assumed to occur with an excited state  $g$  factor of 2 as indicated by Eqs. 2 or 3 then the  $-\frac{1}{2}\rightarrow-\frac{3}{2}$  transition, which has a relative intensity of  $\frac{3}{4}$ , should correspond to a  $g$  factor of about 1.6 in order that the average position corresponds to  $g=1.7$ . The peak height then should be about 75% of that of the  $\frac{1}{2}\rightarrow\frac{1}{2}$  transition. Although the corresponding 25% increase in width of the line might not be observable in the present experiment, the 25% difference in peak heights would be, but is not observed. Since it is likely that the Jahn-Teller effect is operative in the ground state it also affects the excited state when the optical transition takes place vertically on a configuration coordinate diagram. The effect is that the excited-state basis is no longer the cubic one but some linear combination appropriate to the particular Jahn-Teller distortion. Admixture of the two doublets of the  $\Gamma_8$  quartet now occurs and both  $g$  factors may shift from the spin only value.

It is of interest to note that the  $g$  shift in the excited state is to values less than 2. Since the spin-orbit interaction is negative the energy denominator,  $10 Dq$  in Eq. (3), then also has to be negative. This shows that the interaction takes place with a lower-lying level as the simple model indicates. This level has not been observed directly, unless it is responsible for the second and lower energy line in the photoluminescence spectrum observed by Broser *et al.*<sup>3</sup> This splitting is  $\approx 1200 \text{ cm}^{-1}$  in the crystal-field model and the reduction to  $14 \text{ cm}^{-1}$  would have to be a result of the Ham effect.

## V. CONCLUSION

It is clear from the foregoing that the crystal-field model is not adequate to explain quantitatively the observations on the ZnS:Cu infrared spectrum. The angular dependence of the intensities and polarization selection rules of the various transitions is qualitatively in agreement with the model but this data lacks precision and straight-forward interpretation obtained from the  $g$  factors. The model does not explain the observed  $g$  factors, in the sense that essentially complete delocalization is predicted for the electrons in the ground state and the model does not allow for such large effects. The dynamic Jahn-Teller effect, however, may provide the explanation for the large  $g$  shift in the ground state. Furthermore, it is not possible to reconcile the equal Zeeman splitting of the two Kramers doublets in the excited state with the large shift away from the spin only value of 2. The quartet nature of this excited state could only be inferred from the angular dependence of the intensities of the transitions and so is only tentative.

The reason for considering the model in some detail, nevertheless, is that for the other copper centers it is not clear whether the crystal-field model is insufficient. These centers, observed in paramagnetic resonance

spectra of Cu in ZnS and related centers fall roughly into two classes.<sup>2</sup> The first has its Landé  $g$  factor near that of the spin only value of 2. In the second class of centers the orbital contribution to the magnetic moment is reduced by about half and the  $g$  factors are shifted away from 2. The present results are an extreme case of this class of centers.

Figure 8 is a brief summary of the related paramagnetic resonance centers which have been observed<sup>2</sup> and the ZnS:Cu infrared center has been added in this plot of  $g_{11}$  versus  $g_{\perp}$ , since most centers have  $C_{3v}$  symmetry. In particular for ZnO:Cu, which has been studied in most detail,<sup>11</sup> large discrepancies occur only in the hyperfine structure constants and in the spin-orbit-interaction constant. For BeO:Cu there is less data but the observations are consistent with the model,<sup>12</sup> but the spin-orbit interaction could not be calculated from the data. The amount of data is much less for ZnS:Ni,<sup>13</sup> and the analysis of CdS:Cu-A has not included the hfs<sup>14</sup> where the discrepancies might show up. The other paramagnetic resonance centers<sup>2</sup> with  $g$  factors near 2 differ primarily in their hfs constants. Some of these centers must be Cu associates with the paramagnetic electrons localized elsewhere and interacting with the nearby copper to show the Cu hfs in the spectrum. Some of these centers might be paramagnetic substitutional Cu in trigonal symmetry, but none of the centers for which enough data is available has yet been explained in terms of the crystal-field model.

Calculations of the Jahn-Teller effect are very complex for this system especially since the amount of data available is so small. Briefly, when the effect is operative, the orbital triplet  $T_2$  of the  $3d^9$  configuration undergoes a spontaneous distortion.<sup>5,15</sup> There are two distortions of symmetry  $T_2$  and one of symmetry  $E$  which are allowed. If the effect is active in one or more of the spin-resonance Cu centers<sup>2</sup> at least one  $T_2$  distortion is involved since these centers all have  $\langle 111 \rangle$  symmetry axes which are also the directions for the minima when the interaction is with a  $T_2$  vibrational mode. Two cases of static Jahn-Teller effect are known in fourfold coordination<sup>16</sup>: CdS:Cr<sup>2+</sup> and ZnSe:Cr<sup>2+</sup>. The static distortions are along  $\langle 100 \rangle$ -like directions and indicate an  $E$  distortion. The axes of Cr<sup>2+</sup> in eightfold coordination in CaF<sub>2</sub> and CdF<sub>2</sub> are along  $\langle 110 \rangle$ , and indicate a combination of two or more distortions. The case of eightfold coordination is expected to be similar to fourfold coordination since both the distortions and the  $\sigma$

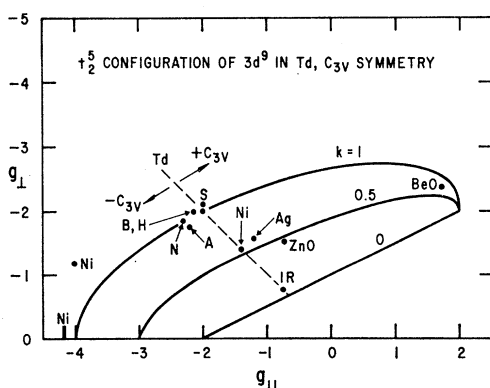


FIG. 8. Summary of paramagnetic centers with a  $3d^9$  configuration in II-VI compounds, plotted as  $g_{11}$  versus  $g_{\perp}$  in  $T_d$  and related  $C_{3v}$  symmetry. The crystal-field model predicts that these quantities be within the ellipse  $k=1$ , the line  $k=0$ , and  $g_{\perp}=0$ , provided the configuration interaction is neglected. The three centers Ni are in ZnS, Ag is in CdS, A and B are CdS:Cu, ZnO and BeO are Cu in these materials. H, N, and S are ZnS:Cu, the point near  $(-2, -2)$  represents a number of other ZnS:Cu centers. The point IR is from the present work.

<sup>12</sup> M. de Wit and A. R. Reinberg, Phys. Rev. **163**, 261 (1967).

<sup>13</sup> M. de Wit, W. C. Holton, T. L. Estle, and J. Schneider, Bull. Am. Phys. Soc. **9**, 249(A) (1964).

<sup>14</sup> K. Morigaki, in *II-VI Semiconducting Compounds, 1967 International Conference*, edited by D. G. Thomas (W. A. Benjamin, Inc., New York, 1967), p. 1348.

<sup>15</sup> R. M. MacFarlane, J. Y. Wong, and M. D. Sturge, Phys. Rev. **166**, 250 (1968).

<sup>16</sup> T. L. Estle, G. K. Walters, and M. de Wit, in *Paramagnetic Resonance*, edited by W. Low (Academic Press Inc., New York, 1963), Vol. I, p. 144; K. Morigaki, J. Phys. Soc. Japan **19**, 187 (1964); M. de Wit, T. L. Estle, W. C. Holton, and A. R. Reinberg, Bull. Am. Phys. Soc. **10**, 329 (1965).

bonding of the  $d$  electrons with their neighbors are similar in the two cases. All four of these centers are static Jahn-Teller distortions and do not result from defect associations, because the populations of the variously oriented centers redistribute themselves when stress is applied at Helium temperatures.<sup>16</sup>

Since the absorption spectrum of ZnS:Cu consists of a single absorption line the various Jahn-Teller distorted centers must interconvert at a rate which is fast compared to the observation time. If this time is related to the linewidth it is less than  $3 \times 10^{-12}$  sec. The spin-orbit interaction provides a coupling between the various distortions, but it is comparable in magnitude to the Jahn-Teller energy and cannot be treated as a perturbation, as can be done for the  $3d^1$  system.<sup>15</sup> A fairly complete calculation is therefore necessary, in which the various vibrational interactions are explored. The number of parameters, therefore, will be large and

much more data for a given defect center will be needed to explain the results in terms of this theory.

Meanwhile, the comparison of the  $g$  factors in optical and paramagnetic resonance work provides the direct link which is needed to correlate the results of the two methods on such centers. The Zeeman splittings of the optical absorption spectrum provide the necessary information to make this connection with future paramagnetic resonance studies of copper-doped ZnS.

#### ACKNOWLEDGMENTS

The author is indebted to F. D. Sinclair for his help in taking the data and to R. Stinedurf and D. Ruthven for the crystal preparation. Discussions with Dr. W. C. Holton and Dr. R. K. Watts have been helpful. Thanks are due to Dr. G. Harkins of the Southwest Center for Advanced Studies for his hospitality.

### Ultrasonic Paramagnetic Resonance of $U^{4+}$ in $CaF_2$ †

PERRY F. McDONALD

*Solid State Physics Branch, Physical Sciences Laboratory, Redstone Arsenal, Alabama 35809*

(Received 3 September 1968)

The spin-phonon interaction between the  $U^{4+}$  ion and the  $CaF_2$  lattice has been investigated using ultrasonic paramagnetic resonance. A spin Hamiltonian is given which predicts the observed asymmetric line shape. A spin-lattice Hamiltonian quadratic in spin is used to interpret the UPR results. The spin-lattice coupling constants  $|G_{11}-G_{12}| = 170 \pm 56$  and  $|G_{14}| = 13.2 \pm 4.4$ , and the ratio  $G_{14}/(G_{11}-G_{12}) = -0.078 \pm 0.01$ , were obtained.

#### I. INTRODUCTION

THE spin-lattice interaction for paramagnetic ions in insulating crystals was first treated successfully by Van Vleck.<sup>1,2</sup> In that theory, the modulation of the electric field by lattice vibrations is coupled to the electron spin through the orbital motion of the electron and the spin-orbit coupling, and the interaction is given by a Hamiltonian quadratic in spin. This spin-lattice Hamiltonian is also, to first order, linearly dependent on the lattice strain, and consequently leads to the one-phonon spin-lattice relaxation process. The Van Vleck theory was applied to the resonant absorption of ultrasonic phonons by paramagnetic ions by Al'tshuler,<sup>3</sup> Mattuck and Strandberg,<sup>4</sup> and Orbach.<sup>5</sup> A thorough review of the theory was given by Tucker.<sup>6</sup>

† Submitted to the University of Alabama in partial fulfillment of the requirements for the Ph.D. degree.

<sup>1</sup> J. H. Van Vleck, *J. Chem. Phys.* **7**, 72 (1939).

<sup>2</sup> J. H. Van Vleck, *Phys. Rev.* **57**, 426 (1940).

<sup>3</sup> S. A. Al'tshuler, B. I. Kochelaev and A. M. Leushin, *Usp. Fiz. Nauk* **75**, 459 (1961) [English transl.: *Soviet Phys.—Usp.* **4**, 880 (1962)].

<sup>4</sup> R. D. Mattuck and M. W. P. Strandberg, *Phys. Rev.* **119**, 1204 (1960).

<sup>5</sup> R. Orbach, Ph.D. thesis, University of California, 1960 (unpublished).

<sup>6</sup> E. B. Tucker, *Proc. IEEE* **53**, 1547 (1965).

The successful generation of microwave-frequency phonons using piezoelectric transducers<sup>7,8</sup> made it possible to study the direct spin-lattice interaction by the injection of a large number of phonons in a narrow frequency range. The resonant absorption of these phonons by the spins is just the inverse of the direct process, spin-lattice relaxation, and is called ultrasonic paramagnetic resonance (UPR). There are two general types of UPR experiments. In the first, an ultrasonic pulse is used to saturate<sup>9-11</sup> the paramagnetic spin system resonance which is being monitored with a standard EPR spectrometer. Jacobsen, Shiren and Tucker<sup>9</sup> were the first to use this technique in the study of the direct process. Accurate values of ratios<sup>11</sup> of spin-lattice coupling constants may be obtained by this method, but the calculation of the individual coupling constants is not usually possible, since that

<sup>7</sup> K. N. Baranski, *Dokl. Akad. Nauk SSSR* **114**, 517 (1957) [English transl.: *Soviet Phys.—Doklady* **2**, 237 (1957)].

<sup>8</sup> H. E. Bömmel and K. Dransfield, *Phys. Rev. Letters* **1**, 234 (1958).

<sup>9</sup> E. H. Jacobsen, N. S. Shiren, and E. B. Tucker, *Phys. Rev. Letters* **3**, 81 (1959).

<sup>10</sup> N. S. Shiren and E. B. Tucker, *Phys. Rev. Letters* **6**, 105 (1961).

<sup>11</sup> M. F. Lewis and A. M. Stoneham, *Phys. Rev.* **164**, 271 (1967).